Title

The *period* gene alters daily and seasonal timing in *Ostrinia nubilalis*

Authors

Jacob N. Dayton[1,2,*] & Erik B. Dopman[1,**]

Affiliations

[1]Department of Biology, Tufts University, Medford, Massachusetts, USA[1]
[2]Lead contact
*Corresponding authors

Correspondence:
Jacob Dayton, Jacob.dayton@tufts.edu and Erik Dopman, Erik.dopman@tufts.edu

Summary

The timing of insects' daily (feeding, movement) and seasonal (diapause, migration) rhythms affects their population dynamics and distribution. Yet, despite their implications for insect conservation and pest management, the genetic mechanisms underlying variation in timing are poorly understood. Prior research in the European corn borer moth (*Ostrinia nubilalis*) associated ecotype differences in seasonal diapause and daily activity with genetic variation at the circadian clock gene *period* (*per*). Here, we demonstrate that populations with divergent allele frequencies at *per* exhibit differences in daily behavior, seasonal development, and the expression of circadian clock genes. Specifically, later daily activity and shortened diapause were associated with a reduction and delay in the abundance of cycling *per* mRNA. CRISPR/Cas9-mediated mutagenesis revealed that *per* and/or an intact circadian clock network were essential for the appropriate timing of daily behavior and seasonal responsiveness. Furthermore, a reduction of *per* gene dosage in *per* heterozygous mutants ($per^{-/+}$) pleiotropically decreased the diapause incidence, shortened post-diapause development, and delayed the timing of daily behavior, in a manner phenotypically reminiscent of wild-type individuals. Altogether, this combination of observational and experimental research strongly suggests that *per* is a master regulator of biological rhythms and may contribute to the observed life cycle differences between bivoltine (two generation) and univoltine (one generation) *O. nubilalis*.

Keywords

diapause, period, circadian clock, insect, post-diapause development, European corn borer

Highlights

- Natural ecotypes with divergent *period* (*per*) genotypes differ in their daily and seasonal responses to photoperiod
- Later daily activity, reduced diapause incidence, and shorter post-diapause development is associated with reduced *per* mRNA abundance
- *per* is essential for short-day recognition and daily timing
- Reduced *per* gene dosage shortened post-diapause development and delayed locomotor activity

Introduction

Most plants and animals face strong selective pressures to synchronize their behavioral, physiological, and reproductive cycles with daily and seasonal changes in the environment. Suboptimal timing of these responses can negatively impact individual fitness and population persistence [1–3]. To counter this, many species have evolved endogenous timing mechanisms that track photoperiod, allowing them to anticipate and respond to rhythmic environmental change.

Insects exhibit photoperiodic diapause, a plastic form of seasonal development comparable to mammalian hibernation. Classical night interruption and resonance experiments have long suggested that the endogenous circadian clock is involved in seasonal photoperiodic time measurement and diapause regulation [4–7]. The circadian clock relies on transcriptional/translational feedback loops [8], and in Lepidoptera, is initiated by the CLOCK (CLK):BMAL1 heterodimer, which drives rhythmic transcription of *period* (*per*), *timeless* (*tim*), and *cryptochrome 2* (*cry2*). In darkness, the resulting TIM, PER, and CRY2 proteins form a complex that translocates into the nucleus to repress CLK:BMAL1-mediated transcription [9–12].

Geographic variation in diapause timing has frequently been associated with both allelic variation in clock genes [13–18] and differences in circadian timing [19–21]. Despite these associations, the functional contribution of variation in the circadian clock to the regulation and evolution of diapause remains understudied [22]. Laboratory manipulations have demonstrated that the circadian clock network is essential for photoperiodic responsiveness in various non-model insects [23–33]. However, these studies often involved only single populations or genotypes [22], which can limit understanding how molecular variation drives population-level divergence. A powerful approach is to combine experimental manipulations with ecologically diverse genotypes [34–37], but this approach has not yet widely been applied to insect diapause studies (but see [13,28,38]).

The European corn borer moth (*Ostrinia nubilalis*) is an agricultural pest that offers an exceptional opportunity to study how genetic variation in circadian clock genes influences behavior and development. Two ecotypes of *O. nubilalis* differ in the number of generations (voltinism) per growing season, largely driven by differences in post-diapause development (PDD) time of overwintering prepupae [39,40]. Kozak et al. (2019) associated non-coding variants that disrupt an E-box motif within the 5'UTR of the *per* gene with the shorter post-diapause development (PDD) time of individuals from a two-generation (bivoltine) ecotype, which also exhibit longer endogenous circadian periods than their one-generation (univoltine) counterparts. Minor gene expression differences between ecotypes were detected for some clock genes [41], but quantitative measurements remain to be estimated for *per* and the rest of the core clock gene network. These findings suggest that variation in *per* genotype and function might contribute to the phenotypic variation in both daily and seasonal traits [42].

Here, we integrate behavioral assays, transcriptome profiling, and targeted genetic/pharmacological manipulations to investigate *per*'s function in both biological rhythms. Our results demonstrate that the circadian clock gene *per* is essential for timekeeping and reductions to *per* gene dosage directly alter both daily and seasonal rhythms. Based on these laboratory results, we hypothesize that *per* genotype-specific differences in *per* transcript abundance may contribute to the ecotype divergence in *O. nubilalis*, offering new insights into how genetic variation in clock genes may shape adaptive responses in insects.

Results and Discussion

Ostrinia nubilalis ecotypes differ in timing.

The relationship between seasonal and daily timing was explored by measuring the prepupal diapause response and overt activity rhythms of univoltine and bivoltine *O. nubilalis* ecotypes with divergent allele frequencies at *period* (*per*). *O. nubilalis* were responsive to subtle changes in photoperiod and reproduced diapause phenotypes previously documented in the field [39,43] and laboratory [42,44]. As daylength decreased, diapause incidence increased, and fewer individuals continuously developed into pupae (Fig. 1A). Genetic variation in the response to photoperiod was reflected by the statistically significant effects of ecotype (i.e., genetic background) and the interaction between ecotype and photoperiod on both diapause incidence and post-diapause development (PDD) time (Fig. 1A-1B; see Fig. S1). The bivoltine ecotype exhibited lower diapause incidence in longer photoperiods (Fig. 1A) and a shorter PDD time after transfer to diapause-breaking conditions (Fig. 1B; see Fig. S1).

Highlighting possible connections between the circadian clock and seasonal timing, a shifted phase (Φ) in the daily timing of peak locomotor activity (Fig. 1C) accompanied these ecotype differences in seasonal diapause. Bivoltine males were active 0.72 hr (Φ, 95% CI: 0.33−1.12 hr) later than univoltine males (normal distribution; $t = 3.74$, $df = 37$, $P = 0.006$; Fig. 1C). Specifically, in *D. melanogaster*, an advanced phase of activity (LD) and a shorter free-running period (DD) reflect earlier PER-mediated transcriptional repression, driven by increased *per* gene dosage [45–47], elevated transcription of *per* [46,48,49] and/or altered phospho-regulation of PER protein stability/abundance and nuclear localization [50–54]. Accordingly, the later activity phase of bivoltine males was consistent with their longer free-running period in DD (Fig. 1D). Although some components of the Lepidopteran circadian clock differ from *D. melanogaster* [8], we hypothesized that these behavioral phenotypes in bivoltine *O. nubilalis* may similarly represent a delay in PER repression, driven by reduced *per* gene expression and/or delayed PER protein accumulation during the evening.

O. nubilalis ecotypes differ in clock gene expression.

To explore potential transcriptional mechanisms underlying ecotype differences, we leveraged 3'-end RNA sequencing [55,56] to quantify cycling gene expression in *O. nubilalis* brains, the site of the central circadian pacemaker and photoperiodic timer [7]. Across a 12L:12D cycle, RNA was isolated from replicate pools of fifth instar diapause-destined brains at 3-hr intervals, starting from the scotophase of day 4 through the photophase of day 5. Although cosinor regression identified 1,230 rhythmic genes (12% of expressed genes), with 773 that were differentially rhythmic [57] between ecotypes ($q_{DR} < 0.05$), we focused our investigation on the expression of the core circadian clock genes in Lepidoptera [8](Fig. 5B).

Within the *O. nubilalis* brain, ecotypes differed in their gene expression profiles for core components of the circadian clock gene network. Later evening activity of bivoltine individuals (Figs. 1C, 1D) was mirrored at the transcriptional level by a 1.4 hr later mean phase (Φ) of cyclic expression of *per, cryptochrome 2* (*cry2*), and *vrille* (*vri*) genes (95% CI: 1.0−1.7 hr; $t = 17.0$, $df = 2$, $P < 0.003$; Fig. 2), all of which were significantly rhythmic in both ecotypes (Fig. 2). Pairwise comparison of these genes revealed significantly lower rhythm-adjusted mean (mesor) expression of *per* ($P = 0.027$) and higher mesor expression of *vri* ($P = 0.001$) in bivoltine individuals (Fig. 2). For the six genes lacking cross-ecotype rhythmicity, *clk* was downregulated

(log_2FC = -0.56, q = 0.004) and both *cyc* (log_2FC = -1.06, q = 0.003) and *tim* (log_2FC = -0.46, q = 0.002) were upregulated in the bivoltine ecotype.

Based on the function of circadian clock genes in *D. melanogaster* [58] and Lepidoptera [8], the reduced expression of *clk* and *per* [9,10,12], paired with upregulated *vri* [59,60], jointly suggested that the bivoltine population's later activity (Fig. 1C) and longer free-running period (Fig. 1D) could be a consequence of reduced evening accumulation of PER and a dose-dependent delay in PER-mediated repression (Fig. 5A-5B). Although the connection between differences in the circadian clock network and seasonal timing is less clear in the literature, the prior association between ecotype variation in diapause responses and *per* genotype[42] suggested that amplifying effects of reduced *per* (Fig. 2) across days may also contribute to the lower diapause propensity (Fig. 1A) and shorter PDD time of bivoltine individuals (Fig. 1B).

Reduced *per* gene dosage confers bivoltine-like responses.

Given that the shorter PDD time of bivoltine *O. nubilalis* (Fig. 1) is associated with genetic variation in the *per* 5' UTR [42] and reduced *per* gene expression (Fig. 2), we leveraged CRISPR/Cas9 to investigate whether *per*/PER abundance directly alters daily behavior and seasonal diapause. Since the number of wild-type *per* gene copies in *D. melanogaster* is inversely correlated with the free-running period length [45–47,61] and *per* mRNA abundance [46], we predicted that reducing *per* gene dosage would similarly decrease the abundance of *per*/PER in *O. nubilalis* and resemble bivoltine-like phenotypes. We generated germline mutants bearing frameshift mutations in *O. nubilalis per* exon four [62], upstream of the predicted Per-Arnt-Sim (PAS) domain. Consistent with reports from other insects [30,31], *per* hemizygous female mutants (*per* $^{-}$/W) were unresponsive to a diapause-inducing photoperiod (see Fig. S2A), and they exhibited arrhythmic adult eclosion behavior (see Fig. S2B), indicative of a dysfunctional circadian clock [11,30,31,63]. In the absence of an *O. nubilalis*-specific PER antibody, these defects suggested that frameshifts at this sgRNA target site resulted in a true loss-of-function allele.

In contrast, *per* heterozygous mutants (*per* $^{-/+}$) were still responsive to photoperiod and exhibited nearly 100% diapause incidence in 12L:12D (Fig. 3A). However, when larvae in a diapause-inductive photoperiod (12L:12D) were exposed to a late-night light pulse, known to accelerate PER degradation [10,64], diapause incidence was drastically reduced (Fig. 3A). Resembling the lower diapause incidence (Fig. 1A) and elevated photosensitivity of bivoltine wild-type *O. nubilalis* (see Fig. S3), *per* heterozygous mutants (*per* $^{-/+}$) with only one functional *per* gene copy were more sensitive to diapause-averting night interruptions (Fig. 3A). This similarity between laboratory mutants and wild-type bivoltine individuals suggested that *per* (and PER repression) may directly be involved in measuring night length, the causal factor determining diapause incidence in *O. nubilalis* [4,65] and many other insects [6,7].

To conservatively isolate the effect of *per* gene dosage from any differences between families, arising from genetic background or a family-specific microenvironment, we reared *per* heterozygous mutants (*per* $^{-/+}$) alongside their respective wild-type (*per* $^{+/+}$) siblings in 12L:12D. Diapausing larvae/prepupae were transferred to 16L:8D to terminate diapause and track PDD to pupation. Indicating a direct link between *per* gene dosage and seasonal timing, PDD time was significantly predicted by *per* gene dosage and family (Fig. 3B), and *per* heterozygous mutants exhibited a 7-day shorter PDD time on average (Fig. 3B).

A complementary experiment investigated the effect of different diapause-inducing photoperiods (15L:9D vs. 12L:12D hr) and *per* gene dosage on PDD time. The absence of an

interaction between *per* gene dosage and photoperiod (F = 0.38, *df* = 1, *P* = 0.539) suggested that photoperiod and *per* independently exert their influence on PDD time (see Fig. S4).

To investigate whether a reduction in *per* gene dosage simultaneously altered the circadian clock network, the daily eclosion of adults was separately monitored in LD or after transfer to DD. Consistent with the period lengthening reported in *Drosophila* with reduced *per* gene dosage[45], the circular mean eclosion time of *per* heterozygous mutants (*per* $^{-/+}$) was significantly delayed in DD (Φ = 0.76 hr) and similarly affected in LD (Φ = 0.77 hr; Fig. 3C). Altogether, the analysis of *per* heterozygous mutants revealed that *per* gene dosage (and unmeasured *per*/PER abundance) directly altered both daily and seasonal timing.

Pharmacological period lengthener reduces diapause incidence.

Mutations in a single clock gene, like *per*, cannot easily be isolated from any effect on the entire circadian clock module [25,28,66]. Therefore, to gather additional evidence that delayed PER repression in the circadian clock alters seasonal timing, we performed pharmacological manipulations of wild-type larvae. In *D. melanogaster* and mammals, lithium lengthens the free-running period of the circadian clock [67–69] by inhibiting GSK-3β/SGG-mediated phosphorylation, which can delay nuclear localization of PER [53]. Based on the longer free-running period and reduced diapause incidence of bivoltine *O. nubilalis* (Fig. 1), we hypothesized that dietary lithium supplementation would decrease diapause incidence in a dose-dependent manner reminiscent of reduced *per* gene dosage in *per* heterozygous mutants (Fig. 3A). Consistent with this prediction, increasing concentrations of lithium decreased diapause incidence in both ecotypes (β = -0.027, z = -2.50, *P* = 0.012; Fig. 4). This effect was more pronounced in the bivoltine population (β = -0.029, z = 1.87, *P* = 0.062; Fig. 4), and may reflect the greater slope change near a population's critical daylength (Fig. 1A).

A possible mechanism for biological rhythm.

Overall, we demonstrate that multivariate trait divergence in daily and seasonal timing (Fig. 1) of *O. nubilalis* ecotypes is associated with *per* genotype [42] and altered expression of cycling *per* mRNA (Fig. 2). Laboratory manipulations predicted to delay PER repression, either by reducing wild-type *per* gene dosage (Fig. 3) or lithium treatment (Fig. 4), induced changes resembling wild-type bivoltine *O. nubilalis*. Although we have not functionally validated the influence of naturally-occurring *per* alleles, this combination of observational and experimental research implicates the hypothesis that variation in the circadian clock network directly modifies both daily and seasonal traits. In the case of *O. nubilalis*, *period* is predicted to be a master regulator of daily and seasonal rhythms: reduced *per* mRNA (and PER) abundance during the evening delays daily activity and contributes to a less intense diapause response (Fig. 5). Moreover, finding that a conserved period lengthener (lithium) also reduces diapause incidence suggests that diverse manipulations of circadian clock properties (e.g., amplitude, phase) can also predictably modify seasonal timing. By extension, manipulations [49,70] or environmental conditions [28,71–73] that increase *per* mRNA and advance evening accumulation of PER may confer earlier activity and a more intense diapause response (Fig. 5).

Nevertheless, we note limitations to our study that will require further work. Although the relationship between *per* mRNA levels and the abundance of its cognate protein are tightly associated in *D. melanogaster* [54], we have not yet quantified in *O. nubilalis* how *per* gene expression directly alters PER protein abundance. Secondly, although empirical associations between nuclear localization of the repressive complex, requisite for PER repression [9], and

evening photosensitivity have been documented in *D. melanogaster* [74], PER immunostaining is needed to resolve the neuroanatomical structure of the clock and to identify the onset of repression in *O. nubilalis*. Similarly, coimmunoprecipitation (CoIP) of PER with CLK:BMAL1 or chromatin (ChIP) could respectively inform when PER sequesters CLK from DNA [12,75] and reveal transcriptional targets mediating different daily and seasonal responses. These targets and their downstream signaling pathways [33] could also be nominated from further analysis of the transcriptomic resources developed here.

Although *per* was the focus of this manuscript, Kozak et al. (2019) also associated differences in seasonal timing with variation in the *Pigment dispersing factor receptor* (*Pdfr*) gene. *Pdfr* was hypostatic to allelic changes at *per* and explained less phenotypic variance in PDD time. However, considering that *Pdfr* encodes the receptor for the neuropeptide PDF [76], and PDF/PDFR signaling interacts with PER [64,77] and TIM [78] to adjust the phase and amplitude of clock neurons under long-day photoperiods [77,79], further exploration of its contribution to daily and seasonal timing in *O. nubilalis* is warranted. Already studies in *Culex pipiens* mosquitoes and *D. melanogaster* have shown that PDF signaling is essential for long day responses, and loss of PDF caused insects reared in long day photoperiods to enter a diapause-like state [25,80–82]. In contrast, PDF knockout prevented diapause induction in *Pyrrhocoris apterus* and *Plautia stali* individuals exposed to short days [83–85]. Therefore, an important question concerns how allelic variation at *Pdfr* may alter PER oscillations and contribute to photoperiodic responses in *O. nubilalis*.

Finally, it will be important to investigate how transferable these results are across populations and species. For example, the hormonal control of diapause regulation is relatively consistent across species that diapause in the same life-cycle stage [7]. However, relationships between diapause timing and either variation in circadian clock properties [20] or in the response to clock gene manipulation [33] are not the same across species. Despite this, continued studies of diapausing insects, spanning diapause strategies, life-cycle stages, and mechanisms of photoperiodic time measurement (*i.e.,* night-length, daylength), might reveal commonalities in how changes to the circadian clock's function drive seasonal adaptation.

In summary, we leverage empirical studies of diverse populations with laboratory manipulations to provide evidence that differences in *per* mRNA abundance contribute to the key differences in seasonal timing of univoltine and bivoltine *O. nubilalis* ecotypes. While we predict that reduced *per* mRNA levels delays evening PER accumulation and PER repression of the circadian clock, the specific mechanisms and their downstream targets require further study. Regardless, these results implicate a link between variation in the circadian clock and adaptive differences in seasonal timing.

Data and Code Availability

Raw sequencing data are being submitted to GEO and a GEO:accession number will be provided when assigned. Processed data and original code are publicly available on GitHub: https://github.com/daytonjn/period_ms_2024 and will be accessible at Zenodo via a DOI before publication. Any additional information required to reanalyze the data reported in this paper is available upon request from the lead contact, Jacob Dayton (dayton.jacob.n@gmail.com).

Acknowledgements

We thank K. McLaughlin for access to critical microinjection equipment, A. Balikian, R. Klusza, A. Murray, J. Paul, and T. Tran and for assistance in the lab, E. Saint-Denis for assisting with tissue dissections, and S. Mirkin, B. Trimmer, and M. Meuti for thoughtful feedback on an early version of the manuscript. The authors acknowledge the Tufts University High-Performance Computing Cluster https://it.tufts.edu/high-performance-computing), which was utilized for the research reported in this manuscript. Figure 5 was generated on BioRender with a license to J.N.D.

Funding Information

E.B.D. acknowledges support from the National Science Foundation (Award #2416175) and Tufts University.

Author Contributions

Conceptualization, J.N.D., E.B.D.; Methodology, Investigation, Formal analysis, Data curation, Writing−initial draft, J.N.D.; Writing−review, J.N.D., E.B.D.; Funding acquisition, E.B.D.

Declaration of Interests

The authors declare no competing interests.

Supplemental Information

Document S1. Figures S1-S4 and Tables S1-S2.

295 **Figure Legends**
296
297 **Fig. 1. *O. nubilalis* ecotypes differ in seasonal and daily rhythms.** (A) Diapause induction in
298 larvae exposed to various light-dark (LD) photoperiods at 23.5˚C. Diapause was determined as
299 the failure to pupate by day 35. Photoperiod (LR χ^2 = 1108, *df* = 1, *P* = <2.2*10^{-16}), ecotype (LR
300 χ^2 = 15.55, *df* = 1, *P* = 8.05e-5), and their interaction (LR χ^2 = 4.99, *df* = 1, *P* = 0.026)
301 significantly predicted diapause incidence (binomial GLM, logit link). Dashed lines denote the
302 Critical Daylength (CDL), where the probability for diapause is 50%, for univoltine (15.05 L) and
303 bivoltine (14.89 L) populations. (B) Diapausing larvae from 14.25L:9.75D were transferred to
304 16L:8D to track post-diapause development (PDD) time to pupation. PDD time was significantly
305 affected by photoperiod (binomial GLM; χ^2 = 123, *df* = 1, *P* < 2.2*10^{-16}), ecotype (χ^2 = 1810, *df*
306 = 2, *P* < 2.2*10^{-16}), and their interaction (χ^2 = 125, *df* = 2, *P* < 2.2*10^{-16}). Bivoltine individuals
307 completed PDD ~20 days earlier than 50% of univoltine individuals (38.5 days). See Fig. S1 for
308 results from other diapause-inducing photoperiods. (C) Across LD photoperiods, the phase of
309 peak locomotor activity was significantly affected by daylength (F = 41.5, *df* = 1, *P* = 1.78*10^{-7})
310 and ecotype (F = 14.0, df = 1, *P* < 0.001), but not their interaction (*P* = 0.291). (D) In continuous
311 darkness (DD), the free-running period length of bivoltine males was 1.4 hr longer (95% CI:
312 0.85−1.95 hr) than univoltine males (*t* = 7.31, *df* = 3.72, *P* = 0.002). Shading denotes 95%
313 confidence intervals. Asterisks denote P < 0.01 (**).
314
315 **Fig. 2. *O. nubilalis* ecotypes differ in rhythmic expression of core circadian clock genes**
316 **in the brain.** Larvae (12L:12D, 23.5˚C) were synchronized at molt into the final 5th instar (day
317 0). Pools of 3-4 brains were dissected every three hours from day 4 (ZT14) through day 5
318 (ZT11). Darkness is shaded (ZT12-24). Across ecotypes, evidence for significant rhythmicity
319 (cycling) in gene expression was evaluated by cosinor regression and adjusted for multiple
320 comparisons (B-H method, *q* value). Asterisks denote q_{rhy} < 0.10 (*), q_{rhy} < 0.05 (**), and q_{rhy} <
321 0.01 (***). Genes that are rhythmic within ecotypes (P_{rhy} < 0.05) are illustrated with solid fitted
322 cosine-regression lines; dotted lines indicate no significant cosine fit curve (P_{rhy} ≥ 0.05).
323 Comparisons of rhythmic genes between ecotypes revealed significant differences in the mesor
324 (*per*, *P* = 0.027; *vri*, *P* = 0.001) and consistent differences in phase (Φ). *clk*, *clock*; *bmal1*, *brain*
325 *and muscle Arntl-like 1*; *cyc*, *cycle*; *cry2*, *cryptochrome 2*; *per*, *period*; *vri*, *vrille*; *tim*, *timeless*;
326 *pdp1-e*, *par domain protein 1*; *cwo*, *clockwork orange*. *Drosophila*-like *cryptochrome 1* is not
327 displayed and was not rhythmic (q_{rhy} > 0.10).
328
329 **Fig. 3. Reduced *per* gene dosage pleiotropically modifies seasonal development and**
330 **daily behavior.** (A) Diapause induction of larvae reared in 12L:12D and exposed to a 1.5 hr
331 night-interruption light pulse (no pulse = 0). Diapause incidence was significantly affected by
332 photoperiod treatment (χ^2 = 131.3, *df* = 4, *P* < 2.2*10^{-16}), genetic background (χ^2 = 44.5, *df* = 1,
333 *P* < 2.57*10^{-11}), and their interaction (χ^2 = 11.2, *df* = 4, *P* = 0.025). Significant differences were
334 evaluated by a two-sample proportion test. Shading denotes 95% confidence intervals.(B, left)
335 Diapausing larvae (12L:12D) were transferred to 16L:8D to track post-diapause development
336 (PDD) time. Each family contained paired *per* homozygous wild-type (*per* $^{+/+}$) and *per*
337 heterozygous mutant (*per* $^{-/+}$) siblings, genotyped by allele-specific PCR or amplicon
338 sequencing. (B, right) Intra-family differences in mean PDD time between heterozygous mutants

and wild-type siblings. Only *per* gene dosage (two-way ANOVA: F = 15.8, *df* = 1, *P* < 0.001) and family (F = 5.51, *df* = 5, *P* < 0.001), but not their interaction (F = 0.54, *df* = 5, *P* = 0.742), significantly predicted PDD time. Averaged across families, *per* heterozygous mutants exhibited a 6.6 day shorter PDD time (95% CI: 3.3−9.9 days, *t* = 4.0, *P* < 0.001). (C) Eclosion of adults from their pupal case in DD (Left) and LD (Right) was binned into 1 hr intervals and pooled across families. (C, left) Pupae were kept in 16L:8D and transferred to continuous darkness (DD) seven days after pupating. (C, right) Pupae were kept in 12L:12D. The lights turned on at Zeitgeber Time 0/24. Arrows denote the circular mean eclosion time, which was delayed in *per* heterozygous mutants in both DD (Φ = 0.76 hr; Watson's Two-sample U^2= 0.215, *P* < 0.05) and LD (Φ = 0.77 hr; U^2 = 0.057, *P* > 0.10). Asterisks denote *P* < 0.05 (*), *P* < 0.01 (**), *P* < 0.001 (***).

Fig. 4. Lithium reduces diapause incidence in *O. nubilalis*. Groups of larvae from bivoltine and univoltine ecotypes were reared in diapause inducing conditions (14.9L:9.1D, 15L:9D). From the onset of the fifth instar, larvae were isolated and fed a diet containing 0, 10, or 25mM of LiCl. The effects of lithium concentration, photoperiod, and background on diapause incidence were analyzed by a binomial GLM using a logit link. Lines denote model predicted diapause incidence for each combination of fixed effects. Diapause incidence was significantly affected by ecotype (binomial GLM; χ^2 = 216, *df* = 1, *P* = 2.2*10-16) and photoperiod (χ^2 = 12.45, *df* = 1, *P* < 0.001), with evidence for a lesser effect by lithium (χ^2 = 2.914, *df* = 1, *P* = 0.088) and the interaction between ecotype and concentration (χ^2 = 3.53, *df* = 1, *P* = 0.060). Each point represents a replicate group (28-30 larvae). Shading denotes 95% confidence intervals.

Fig. 5. *per* transcript abundance alters daily and seasonal rhythms in *O. nubilalis*. (A) Variation in the phase (Φ) or amplitude of *per* mRNA abundance, and predicted PER protein accumulation, across a 24-hr day is associated with differences in daily behavior and seasonal development of univoltine (red) and bivoltine (blue) individuals. (B) In a simplified model of the Lepidopteran circadian clock network[8], we hypothesize that earlier vs. later repression of CLK:BMAL1 in the evening (scotophase) pleiotropically alters both daily and seasonal rhythms of wild-type individuals. (C) Experimental reductions in *per* gene dosage (blue) delay the phase of daily behavior, decrease photoperiodic diapause incidence, and shorten post-diapause development (PDD).

STAR Methods

Insect stocks

Univoltine and bivoltine European corn borers (ECB; *Ostrinia nubilalis*) were collected from laboratory populations maintained at Tufts University (Medford, MA). These colonies were originally derived from insects collected in corn stubble in New York, USA and New Hampshire, USA. These colonies have repeatedly been selected for univoltine vs. bivoltine PDD-time[42] and exhibit divergent allele frequencies at *per*. As described previously[62], *O. nubilalis* larvae were reared on artificial corn borer diet (Southland Products, USA) and maintained in an environmental room at 16L:8D (25.5˚C; 55% RH).

Phenotyping diapause in wild-type individuals

To induce diapause, eggs were suspended over diet and reared in climate-controlled incubators for 12L:12D hr at 23.5˚C (50% RH). Fourteen days after hatching, larvae were transferred into individual diet-containing 1.25 oz plastic souffle cups and transferred to various photoperiods differing in the duration of photophase. Photoperiodic response curves for diapause incidence were derived from individuals exposed to 14.25L:9.75D, 14.75L:9.25D, 15.25L:8.75D, and 16.5L:7.5D hr. Larvae who failed to pupate before Day 35 were classified as diapausing [86,87]; by this day, the cumulative pupation curve has already leveled off. On Day 35, larvae were transferred to 16L:8D to artificially terminate diapause [42]. To score PDD-time, individuals were checked every two days for pupation.

Phenotyping diapause in response to night-interruption by light

Experiments predominantly utilized bivoltine and univoltine larvae. To test the influence of *per* gene dosage on diapause incidence, a bivoltine *per* hemizygous mutant female (*per* $^{-}$*/W*) was crossed with a wild-type univoltine male to generate *per* heterozygous mutants (*per* $^{-/+}$) and wild-type females (*per* $^{+}$*/W*). Larvae were initially reared from hatching in a photoperiod known to induce diapause (12L:12D hr at 26˚C). After 14 days, larvae were isolated into individual cups with diet and transferred into various night interruption treatments to determine the position of the photoinducible phase [6,88]. Night interruption treatments were conducted in opaque boxes with overhead warm white LED strip lights. LED lights were programmed with either BN-LINK or myTouchSmart digital outlet timers. Every treatment box contained 48 individuals. A black towel covered boxes to prevent any light from escaping.

Night interruption experiments consisted of a 12L:*x*D:*y*:(12-*x*-*y*)L hr photoperiod (T=24), with *x* denoting the onset of the interruption light and *y* denoting the duration of the light pulse [89]. The larvae were maintained in night interruption treatments for 16 days. Individuals who failed to pupate by day 32 were considered in diapause. Larvae that did not survive the length of the experiment were not included in the results. One bivoltine family was completely non-diapausing and pupated under all photoperiods; these were removed from analyses. The effects of genetic background, night interruption timing (factor), and their interaction on diapause incidence were modeled by a binomial GLM with a logit link. Significant differences in diapause incidence were evaluated by two-sample proportion tests.

Phenotyping diapause in *per* mutant families

Offspring of different *per* heterozygous mutant males and wild-type females were exposed to either 12L:12D hr (Families A-F) or 15L:9D hr (Families E-F) at 23.5˚C. After 35-42 days in inducing conditions, diapausing larvae were transferred to 18˚C for 7 days and then stored at 4˚C for 45 days. To terminate diapause and promote post-diapause development,

larvae were transferred to 16L:8D and checked every two days for pupation. Quiescent larvae that rapidly pupated within eight days were excluded from analyses. The experiment was initially run in 2022 (Families A-D) and repeated in 2024 (Families E-F).

Effect of pharmacologic period-lengthening on diapause induction

European corn borer larvae were reared in 14.9L:9.1D and 15L:9D hr (23.5˚C) . Upon head-capsule slippage preceding molt to 5th instar, larvae were removed from their artificial diet (Southland Products), transferred into one of two photoperiodic conditions previously shown to induce diapause in 50% of the population (14.9:9.1 LD and 15:9 LD hr), and placed onto fresh diet containing an additive. Larvae who failed to pupate by day 35 were considered in diapause. At this temperature, the cumulative pupation curve has already leveled off in a control population. The experiment was separately conducted with bivoltine (Fall 2020) and univoltine (Spring 2021) individuals. Across both experiments, 3-4 replicate groups of 30 larvae were exposed to various LiCl concentrations (0mM, 10mM, 25mM LiCl). The effects of pharmacologic treatment and photoperiod on diapause incidence were determined by a binomial regression with a logit link. Anova() in the *car* package evaluated significance for effects and interactions.

Phenotyping eclosion

Eclosion was monitored by the Raspberry Pi-based imaging Locomotor Activity Monitor [90], as previously described in Dayton et al. (2024). The only modifications were that in 2022, pupae from Families A-D were transferred into continuous darkness seven days after pupation. In 2024, pupae from Families E-F were transferred upon pupation into 12L:12D and monitored for eclosion in LD.

Phenotyping locomotor activity

The imaging Locomotor Activity Monitor (iLAM)[90] quantified locomotor activity of adult males exposed to entraining (LD) and free-running (DD) conditions. Activity of three replicate flight cages containing four to five males each was recorded for 4-5 days in an enclosed room at 23˚C (40% RH). For LD experiments, paired flight cages were exposed to 12L:12D, 14L:10D, 15L:9D, or 16L:8D hr photoperiods by connecting overhead LED lights (3000K Warm White, Pautix) to programmed outlet timers (BN-LINK). Individual photoperiod conditions were isolated from each other by multiple blackout curtains. The time that lights turned on was synchronized across cages and denoted as Zeitgeber Time 0 (ZT0). For circadian phenotyping in DD, moths were acclimated in flight cages for one day in 16L:8D before exposure to DD.

Image segmentation and movement quantification utilized the *iLAMtools* wrapper functions [90] for *imager* [91]. All analyses occurred in the *Rethomics* [92] framework. Activity in LD was smoothed with a Butterworth filter and *pracma* [93] identified the daily timing of peak activity. Free-running period length (DD) was estimated by chi-squared periodogram.

RNA library preparation and sequencing

Diapause-destined *O. nubilalis* larvae (12L:12D, 23.5˚C) from univoltine and bivoltine ecotypes were staged at molt into the final 5th instar (day 0). Beginning on the fourth day of the fifth instar, four replicate pools of 3-4 brains each were isolated every three hours from Day 4 (ZT14) through Day 5 (ZT11). Larvae were decapitated and brains were dissected in DNA/RNA Shield (Zymo Research, R110050) reagent and frozen at -20˚C. To avoid batch effects due to differences in RNA purification efficiencies, all homogenized samples were purified in parallel using the Quick-RNA MicroPrep Kit (Zymo Research, R1050). Total RNA was eluted in water, quantified with the NanoDrop and diluted to ~20ng/uL. To avoid batch effects in cDNA

amplification and library preparation, we prepared a high-throughput Mercurius BRB-seq 3'-mRNA library (Alithea Genomics, 10813) following manufacturer's instructions, with ~200ng RNA from each sample. Cleanup and concentration steps used HighPrep PCR magnetic beads (MagBio Genomics, AC-60005). Tagmentation with pre-loaded adapters used 50ng of cDNA incubated for 8 minutes at 55˚C. Only 12 cycles were used for library indexing and amplification. Sequencing was performed by the Tufts University Core Facility Genomics and used the Illumina NovaSeq XPlus system (1.5B flow cell).

Transcriptomics data analyses

The *Ostrinia nubilalis* reference genome (GCA_963855985.1) was indexed by STAR (2.7.11b) [94] using the RefSeq Genes annotation track (GCF_963855985.1) with rRNA genes removed (gene_biotype "rRNA"). Raw sequencing reads for all 64 samples were aligned to the genome by STARsolo in alignReads mode following BRB-seq recommendations, except --*outFilterScoreMinOverLread 0.3*, --*outFilterMatchNminOverLread 0.3*. Uniquely mapped reads that overlapped genes were counted using the STARsolo output. Sample Assignment of the total raw reads to individual samples was high, and 88.2% of the reads containing valid barcodes (n = 936,026,352 reads). The quality of the sequencing data was robust, with 96.9% of the bases in cell barcodes and UMIs and 94.8% of the bases in RNA reads having a score ≥Q30. In terms of alignment, 62.2% of the reads mapped uniquely to the reference genome, and 66.9% of these reads overlapped with unique gene features. Of the 17,376 total annotated non-rRNA genes in ECB, 15,155 genes were detected in at least one sample. To remove inconsistently expressed genes across sample timepoints and backgrounds, only genes with at least 0.50 counts per million (CPM) in 25% of samples were retained for further analyses. This resulted in 10,079 genes. All analyses were performed after converting gene counts to logarithmic space via the transformation Log_2(CPM+1). Samples with <300,000 reads assigned to the genes were excluded from the analysis. Consequently, the number of raw reads assigned per sample ranged from 527,582 to 27,630,712 (mean: 9,582,975). Gene count tables were quantile normalized with the *voom* function from *limma* v3.32.5 [95]. Significantly rhythmic (i.e., cycling) genes, differentially rhythmic, and differentially expressed genes were identified using a cosinor regression in LimoRhyde [57]. Differences in amplitude, phase, and mesor (rhythm-adjusted mean) were further investigated for candidate circadian clock genes by *CircaCompare* [96]. To control false discovery rate, *p* values were converted to *q*-values using the Benjamini and Hochberg (1995) method. Gene orthologs were identified by reciprocal protein BLAST [97] of *O. nubilalis* RefSeq proteins (GCF_963855985.1) and *D. plexippus* (GCF_009731565.1; see Table S1).

CRISPR/Cas9 mutagenesis and mutant genotyping

CRISPR/Cas9 mutagenesis was performed as described previously [62]. Briefly, early-stage embryos were injected with single sgRNA ribonucleoprotein (RNP) complexes targeting *per* (exon 4; see Table S2). DNA was extracted in a 1x DirectPCR tail lysis buffer (Viagen Biotech) containing 1 µg of Proteinase K (ThermoFisherScientific, USA) in a total volume of 100 µL. Samples were incubated for 16 hr at 56˚C and 85˚C for 25 min. Germline mutants harboring a frameshift mutation were verified by PCR and Sanger sequencing (Eton Bioscience).

Experimental individuals were genotyped by allele-specific PCR for known frameshift mutations (Family A-D; Table S1). To limit amplification of the wild-type allele, mutant allele-specific primers were designed with an additional mismatch in the first five bases of the 3' end.

In general, PCRs contained 1X GoTaq Master Mix (Promega), 0.1 µM of mutant allele-specific primers, 0.1 µM of locus-specific primers (positive control for DNA quality), and 1.5 µL of DNA extract in 20 µL.

To increase throughput, insects from Family E-F were genotyped by amplicon sequencing [98]. Briefly, the first round of PCR with gene-specific primers was 20 cycles and gene-specific amplicons were diluted ten-fold before barcoding. Barcoded amplicons were purified using HighPrep PCR magnetic beads (MagBio Genomics, AC-60005) before Illumina preparation and sequencing (Amplicon-EZ service at Genewiz by Azenta). All oligos were synthesized by Integrated DNA Technologies and Eton Bioscience (Table S2).

Genomic reads were trimmed using TrimGalore to remove Illumina adapters and low-quality bases. CutAdapt v.3.7 [99] demultiplexed trimmed sequences by internal barcodes (-e 0.1). Due to overlapping paired-end reads, reads were merged by NGmerge v.0.3 [100] with modified settings (-v -d -m 50). Merged sequences smaller than 110 bases were removed by Seqtk v.75. HISAT2 [101] and aligned to a subset of the *O. nubilalis* reference genome (GCA_963855985.1) containing only the predicted amplicons. HISAT2 trimmed the 5' linker and primer sequences from both 5' and 3' ends (--trim5 37 --trim3 37) of the merged reads, before aligning (-k 1 –score-min L,0,-0.6 --no-spliced-alignment). Alignments in BAM format were sorted and indexed by samtools v.1.2.0 [102]. SNPs and small indels (<50 bp) were called using the GATK4 HaplotypeCaller [103] for females (--sample-ploidy 1) and males/unknown sex (--sample-ploidy 2). GVCFs were combined by *CombineGVCFs* and *GenotypeGVCFs* performed joint genotyping. *VariantFiltration* hard filtered variants by (QD < 2.0 || QUAL < 30 || MQ < 40.0). SNPs were selected and filtered to remove uninformative variants (AF <= 0.15 || AF >= 0.85).

VCFs were parsed into R by *vcfR* v.1.15.0 [104]. For each sample genotype, allele balance was calculated as the proportion of allele counts for the alternate alleles. Heterozygous genotypes with an allele balance (AB) < 0.2 or AB > 0.8 were respectively filtered to homozygous for the reference or alternate allele [105]. To conservatively remove false homozygotes, any genotypes with an allele depth (DP) < 5 were filtered to NA.

Statistical Analyses

All statistical analyses were conducted in R[106]. The effects of genetic background and/or photoperiod on diapause incidence and cumulation pupation were quantified by a binomial logistic regression with a logit link. Linear regression evaluated the effects of period mutation on PDD-time and mass. To account for uneven sampling among families, square root transformed sum contrasts for family, period mutation, and LD photoperiod were used to understand how each factor level deviated from the overall mean. Differences in the distribution of adult eclosion were compared using Watson's U^2 test within the circular package[107]. All regression models were built in lme4 and used *Anova*() from the *car* package[108] to determine the significance of main effects. Significant differences between group proportions and means were respectively evaluated by Wald's Z test and Welch's T test.

References

1. Møller, A.P., Rubolini, D., and Lehikoinen, E. (2008). Populations of migratory bird species that did not show a phenological response to climate change are declining. Proc. Natl. Acad. Sci. U. S. A. *105*, 16195–16200.
2. Michielini, J.P., Dopman, E.B., and Crone, E.E. (2021). Changes in flight period predict trends in abundance of Massachusetts butterflies. Ecol. Lett. *24*, 249–257.
3. Gilbert, N.A., McGinn, K.A., Nunes, L.A., Shipley, A.A., Bernath-Plaisted, J., Clare, J.D.J., Murphy, P.W., Keyser, S.R., Thompson, K.L., Maresh Nelson, S.B., et al. (2023). Daily activity timing in the Anthropocene. Trends Ecol. Evol. *38*, 324–336.
4. Bonnemaison, L. (1978). Effets de l'obscurité et de la lumière sur la diapause d'Ostrinia nubilalis Hbn. (Lép., Pyralididae). Z. Angew. Entomol. *86*, 57–67.
5. Beck, S.D. (1988). Resonance in photoperiodic regulation of larval diapause in Ostrinia nubilalis. J. Insect Physiol. *34*, 929–933.
6. Saunders, D.S. (2020). Dormancy, Diapause, and the Role of the Circadian System in Insect Photoperiodism. Annu. Rev. Entomol. *65*, 373–389.
7. Denlinger, D.L. (2022). Insect diapause (Cambridge University Press).
8. Brady, D., Saviane, A., Cappellozza, S., and Sandrelli, F. (2021). The Circadian Clock in Lepidoptera. Front. Physiol. *12*, 776826.
9. Chang, D.C., McWatters, H.G., Williams, J.A., Gotter, A.L., Levine, J.D., and Reppert, S.M. (2003). Constructing a feedback loop with circadian clock molecules from the silkmoth, Antheraea pernyi. J. Biol. Chem. *278*, 38149–38158.
10. Zhu, H., Sauman, I., Yuan, Q., Casselman, A., Emery-Le, M., Emery, P., and Reppert, S.M. (2008). Cryptochromes define a novel circadian clock mechanism in monarch butterflies that may underlie sun compass navigation. PLoS Biol. *6*, e4.
11. Zhang, Y., Markert, M.J., Groves, S.C., Hardin, P.E., and Merlin, C. (2017). Vertebrate-like CRYPTOCHROME 2 from monarch regulates circadian transcription via independent repression of CLOCK and BMAL1 activity. Proc. Natl. Acad. Sci. U. S. A. *114*, E7516–E7525.
12. Zhang, Y., Iiams, S.E., Menet, J.S., Hardin, P.E., and Merlin, C. (2022). TRITHORAX-dependent arginine methylation of HSP68 mediates circadian repression by PERIOD in the monarch butterfly. Proc. Natl. Acad. Sci. U. S. A. *119*, e2115711119.
13. Tauber, E., Zordan, M., Sandrelli, F., Pegoraro, M., Osterwalder, N., Breda, C., Daga, A., Selmin, A., Monger, K., Benna, C., et al. (2007). Natural selection favors a newly derived timeless allele in Drosophila melanogaster. Science *316*, 1895–1898.
14. Paolucci, S., Salis, L., Vermeulen, C.J., Beukeboom, L.W., and van de Zande, L. (2016). QTL analysis of the photoperiodic response and clinal distribution of period alleles in Nasonia vitripennis. Mol. Ecol. *25*, 4805–4817.
15. Pegoraro, M., Zonato, V., Tyler, E.R., Fedele, G., Kyriacou, C.P., and Tauber, E. (2017). Geographical analysis of diapause inducibility in European Drosophila melanogaster populations. J. Insect Physiol. *98*, 238–244.
16. Pruisscher, P., Nylin, S., Wheat, C.W., and Gotthard, K. (2021). A region of the sex chromosome associated with population differences in diapause induction contains highly divergent alleles at clock genes. Evolution *75*, 490–500.
17. Lindestad, O., Nylin, S., Wheat, C.W., and Gotthard, K. (2022). Local adaptation of life cycles in a butterfly is associated with variation in several circadian clock genes. Mol. Ecol. *31*, 1461–1475.
18. Yu, Y., Huang, L.-L., Xue, F.-S., and Dopman, E.B. (2023). Partial reuse of circadian clock genes along parallel clines of diapause in two moth species. Mol. Ecol. https://doi.org/10.1111/mec.16940.
19. Lankinen, P. (1986). Geographical variation in circadian eclosion rhythm and photoperiodic adult diapause inDrosophila littoralis. Journal of Comparative Physiology A *159*, 123–142.

20. Hut, R.A., Paolucci, S., Dor, R., Kyriacou, C.P., and Daan, S. (2013). Latitudinal clines: an evolutionary view on biological rhythms. Proc. Biol. Sci. *280*, 20130433.
21. Paolucci, S., Dalla Benetta, E., Salis, L., Doležel, D., van de Zande, L., and Beukeboom, L.W. (2019). Latitudinal Variation in Circadian Rhythmicity in Nasonia vitripennis. Behav. Sci. *9*. https://doi.org/10.3390/bs9110115.
22. Ragland, G.J., Armbruster, P.A., and Meuti, M.E. (2019). Evolutionary and functional genetics of insect diapause: a call for greater integration. Curr Opin Insect Sci *36*, 74–81.
23. Ikeno, T., Tanaka, S.I., Numata, H., and Goto, S.G. (2010). Photoperiodic diapause under the control of circadian clock genes in an insect. BMC Biol. *8*, 116.
24. Ikeno, T., Numata, H., and Goto, S.G. (2011). Circadian clock genes period and cycle regulate photoperiodic diapause in the bean bug Riptortus pedestris males. J. Insect Physiol. *57*, 935–938.
25. Meuti, M.E., Stone, M., Ikeno, T., and Denlinger, D.L. (2015). Functional circadian clock genes are essential for the overwintering diapause of the Northern house mosquito, Culex pipiens. J. Exp. Biol. *218*, 412–422.
26. Mukai, A., and Goto, S.G. (2016). The clock gene period is essential for the photoperiodic response in the jewel wasp Nasonia vitripennis (Hymenoptera: Pteromalidae). Appl. Entomol. Zool. (Jpn.) *51*, 185–194.
27. Omura, S., Numata, H., and Goto, S.G. (2016). Circadian clock regulates photoperiodic responses governed by distinct output pathways in the bean bug, Riptortus pedestris. Biol. Rhythm Res. *47*, 937–945.
28. Dalla Benetta, E., Beukeboom, L.W., and van de Zande, L. (2019). Adaptive Differences in Circadian Clock Gene Expression Patterns and Photoperiodic Diapause Induction in Nasonia vitripennis. Am. Nat. *193*, 881–896.
29. Iiams, S.E., Lugena, A.B., Zhang, Y., Hayden, A.N., and Merlin, C. (2019). Photoperiodic and clock regulation of the vitamin A pathway in the brain mediates seasonal responsiveness in the monarch butterfly. Proc. Natl. Acad. Sci. U. S. A. *116*, 25214–25221.
30. Ikeda, K., Daimon, T., Shiomi, K., Udaka, H., and Numata, H. (2021). Involvement of the Clock Gene Period in the Photoperiodism of the Silkmoth Bombyx mori. Zoolog. Sci. *38*, 523–530.
31. Tobita, H., and Kiuchi, T. (2022). Knockouts of positive and negative elements of the circadian clock disrupt photoperiodic diapause induction in the silkworm, Bombyx mori. Insect Biochem. Mol. Biol. *149*, 103842.
32. Liu, X., Cai, L., Zhu, L., Tian, Z., Shen, Z., Cheng, J., Zhang, S., Li, Z., and Liu, X. (2023). Mutation of the clock gene timeless disturbs diapause induction and adult emergence rhythm in Helicoverpa armigera. Pest Manag. Sci. *79*, 1876–1884.
33. Goto, S.G. (2023). Molecular Mechanisms of Photoperiodism. In Insect Chronobiology (Springer Nature Singapore), pp. 271–291.
34. Manceau, M., Domingues, V.S., Mallarino, R., and Hoekstra, H.E. (2011). The developmental role of Agouti in color pattern evolution. Science *331*, 1062–1065.
35. Bendesky, A., Kwon, Y.-M., Lassance, J.-M., Lewarch, C.L., Yao, S., Peterson, B.K., He, M.X., Dulac, C., and Hoekstra, H.E. (2017). The genetic basis of parental care evolution in monogamous mice. Nature *544*, 434–439.
36. Wucherpfennig, J.I., Howes, T.R., Au, J.N., Au, E.H., Roberts Kingman, G.A., Brady, S.D., Herbert, A.L., Reimchen, T.E., Bell, M.A., Lowe, C.B., et al. (2022). Evolution of stickleback spines through independent cis-regulatory changes at HOXDB. Nat. Ecol. Evol. *6*, 1537–1552.
37. Shahandeh, M.P., Abuin, L., Lescuyer De Decker, L., Cergneux, J., Koch, R., Nagoshi, E., and Benton, R. (2024). Circadian plasticity evolves through regulatory changes in a neuropeptide gene. Nature, 1–9.
38. Sandrelli, F., Tauber, E., Pegoraro, M., Mazzotta, G., Cisotto, P., Landskron, J.,

Stanewsky, R., Piccin, A., Rosato, E., Zordan, M., et al. (2007). A molecular basis for natural selection at the timeless locus in Drosophila melanogaster. Science *316*, 1898–1900.

39. Showers, W.B., Chiang, H.C., Keaster, A.J., Hill, R.E., Reed, G.L., Sparks, A.N., and Musick, G.J. (1975). Ecotypes of the European Corn Borer in North America. Environ. Entomol. *4*, 753–760.
40. Mason, C.E., Sappington, T.W., and National Institute of Food and Agriculture (U.S.) (2018). European Corn Borer: Ecology, Management, Association with Other Corn Pests (Iowa State University Extension and Outreach).
41. Levy, R.C., Kozak, G.M., and Dopman, E.B. (2018). Non-pleiotropic coupling of daily and seasonal temporal isolation in the European corn borer. Genes (Basel) *9*. https://doi.org/10.3390/genes9040180.
42. Kozak, G.M., Wadsworth, C.B., Kahne, S.C., Bogdanowicz, S.M., Harrison, R.G., Coates, B.S., and Dopman, E.B. (2019). Genomic Basis of Circannual Rhythm in the European Corn Borer Moth. Curr. Biol. *29*, 3501–3509.e5.
43. McLeod, D.G.R. (1978). Genetics of diapause induction and termination in the European corn borer, Ostrinia nubilalis (Lepidoptera: Pyralidae), in southwestern Ontario. Can. Entomol. *110*, 1351–1353.
44. Skopik, S.D., and Takeda, M. (1987). Diapause induction and termination: north-south strain differences in Ostrinia nubilalis. J. Biol. Rhythms *2*, 13–22.
45. Smith, R.F., and Konopka, R.J. (1982). Effects of dosage alterations at the per locus on the period of the circadian clock of Drosophila. Mol. Gen. Genet. *185*, 30–36.
46. Baylies, M.K., Bargiello, T.A., Jackson, F.R., and Young, M.W. (1987). Changes in abundance or structure of the per gene product can alter periodicity of the Drosophila clock. Nature *326*, 390–392.
47. Levine, J.D., Sauman, I., Imbalzano, M., Reppert, S.M., and Jackson, F.R. (1995). Period protein from the giant silkmoth Antheraea pernyi functions as a circadian clock element in Drosophila melanogaster. Neuron *15*, 147–157.
48. Hardin, P.E., Hall, J.C., and Rosbash, M. (1990). Feedback of the Drosophila period gene product on circadian cycling of its messenger RNA levels. Nature *343*, 536–540.
49. Kadener, S., Menet, J.S., Schoer, R., and Rosbash, M. (2008). Circadian transcription contributes to core period determination in Drosophila. PLoS Biol. *6*, e119.
50. Zerr, D.M., Hall, J.C., Rosbash, M., and Siwicki, K.K. (1990). Circadian fluctuations of period protein immunoreactivity in the CNS and the visual system of Drosophila. J. Neurosci. *10*, 2749–2762.
51. Edery, I., Zwiebel, L.J., Dembinska, M.E., and Rosbash, M. (1994). Temporal phosphorylation of the Drosophila period protein. Proc. Natl. Acad. Sci. U.S.A. *91*, 2260–2264.
52. Bae, K., and Edery, I. (2006). Regulating a circadian clock's period, phase and amplitude by phosphorylation: insights from Drosophila. J. Biochem. *140*, 609–617.
53. Ko, H.W., Kim, E.Y., Chiu, J., Vanselow, J.T., Kramer, A., and Edery, I. (2010). A hierarchical phosphorylation cascade that regulates the timing of PERIOD nuclear entry reveals novel roles for proline-directed kinases and GSK-3beta/SGG in circadian clocks. J. Neurosci. *30*, 12664–12675.
54. Chiu, J.C., Ko, H.W., and Edery, I. (2011). NEMO/NLK phosphorylates PERIOD to initiate a time-delay phosphorylation circuit that sets circadian clock speed. Cell *145*, 357–370.
55. Alpern, D., Gardeux, V., Russeil, J., Mangeat, B., Meireles-Filho, A.C.A., Breysse, R., Hacker, D., and Deplancke, B. (2019). BRB-seq: ultra-affordable high-throughput transcriptomics enabled by bulk RNA barcoding and sequencing. Genome Biol. *20*, 71.
56. Litovchenko, M., Meireles-Filho, A.C.A., Frochaux, M.V., Bevers, R.P.J., Prunotto, A., Anduaga, A.M., Hollis, B., Gardeux, V., Braman, V.S., Russeil, J.M.C., et al. (2021).

Extensive tissue-specific expression variation and novel regulators underlying circadian behavior. Sci Adv *7*. https://doi.org/10.1126/sciadv.abc3781.

57. Singer, J.M., and Hughey, J.J. (2019). LimoRhyde: A flexible approach for differential analysis of rhythmic transcriptome data. J. Biol. Rhythms *34*, 5–18.
58. Patke, A., Young, M.W., and Axelrod, S. (2020). Molecular mechanisms and physiological importance of circadian rhythms. Nat. Rev. Mol. Cell Biol. *21*, 67–84.
59. Blau, J., and Young, M.W. (1999). Cycling vrille Expression Is Required for a Functional Drosophila Clock. Cell *99*, 661–671.
60. Cyran, S.A., Buchsbaum, A.M., Reddy, K.L., Lin, M.-C., Glossop, N.R.J., Hardin, P.E., Young, M.W., Storti, R.V., and Blau, J. (2003). vrille, Pdp1, and dClock form a second feedback loop in the Drosophila circadian clock. Cell *112*, 329–341.
61. Coté, G.G., and Brody, S. (1986). Circadian rhythms in Drosophila melanogaster: analysis of period as a function of gene dosage at the per (period) locus. J. Theor. Biol. *121*, 487–503.
62. Dayton, J.N., Tran, T.T., Saint-Denis, E., and Dopman, E.B. (2024). Efficient CRISPR/Cas9-mediated genome editing in the European corn borer, Ostrinia nubilalis. Insect Mol. Biol. https://doi.org/10.1111/imb.12959.
63. Markert, M.J., Zhang, Y., Enuameh, M.S., Reppert, S.M., Wolfe, S.A., and Merlin, C. (2016). Genomic access to monarch migration using TALEN and CRISPR/Cas9-mediated targeted Mutagenesis. G3 (Bethesda) *6*, 905–915.
64. Li, Y., Guo, F., Shen, J., and Rosbash, M. (2014). PDF and cAMP enhance PER stability in Drosophila clock neurons. Proc. Natl. Acad. Sci. U. S. A. *111*, E1284–E1290.
65. Beck, S.D. (1962). Photoperiodic induction of diapause in an insect. Biol. Bull. *122*, 1–12.
66. Emerson, K.J., Bradshaw, W.E., and Holzapfel, C.M. (2009). Complications of complexity: integrating environmental, genetic and hormonal control of insect diapause. Trends Genet. *25*, 217–225.
67. Padiath, Q.S., Paranjpe, D., Jain, S., and Sharma, V.K. (2004). Glycogen synthase kinase 3beta as a likely target for the action of lithium on circadian clocks. Chronobiol. Int. *21*, 43–55.
68. Dokucu, M.E., Yu, L., and Taghert, P.H. (2005). Lithium- and valproate-induced alterations in circadian locomotor behavior in Drosophila. Neuropsychopharmacology *30*, 2216–2224.
69. Li, J., Lu, W.-Q., Beesley, S., Loudon, A.S.I., and Meng, Q.-J. (2012). Lithium impacts on the amplitude and period of the molecular circadian clockwork. PLoS One *7*, e33292.
70. Rivas, G.B.S., Zhou, J., Merlin, C., and Hardin, P.E. (2021). CLOCKWORK ORANGE promotes CLOCK-CYCLE activation via the putative Drosophila ortholog of CLOCK INTERACTING PROTEIN CIRCADIAN. Curr. Biol. *31*, 4207–4218.e4.
71. Majercak, J., Sidote, D., Hardin, P.E., and Edery, I. (1999). How a circadian clock adapts to seasonal decreases in temperature and day length. Neuron *24*, 219–230.
72. Goto, S.G., and Denlinger, D.L. (2002). Short-day and long-day expression patterns of genes involved in the flesh fly clock mechanism: period, timeless, cycle and cryptochrome. J. Insect Physiol. *48*, 803–816.
73. Menegazzi, P., Vanin, S., Yoshii, T., Rieger, D., Hermann, C., Dusik, V., Kyriacou, C.P., Helfrich-Förster, C., and Costa, R. (2013). Drosophila clock neurons under natural conditions. J. Biol. Rhythms *28*, 3–14.
74. Shafer, O.T., Levine, J.D., Truman, J.W., and Hall, J.C. (2004). Flies by night: Effects of changing day length on Drosophila's circadian clock. Curr. Biol. *14*, 424–432.
75. Menet, J.S., Abruzzi, K.C., Desrochers, J., Rodriguez, J., and Rosbash, M. (2010). Dynamic PER repression mechanisms in the Drosophila circadian clock: from on-DNA to off-DNA. Genes Dev. *24*, 358–367.
76. Renn, S.C., Park, J.H., Rosbash, M., Hall, J.C., and Taghert, P.H. (1999). A pdf neuropeptide gene mutation and ablation of PDF neurons each cause severe abnormalities

of behavioral circadian rhythms in Drosophila. Cell *99*, 791–802.
77. Vaze, K.M., and Helfrich-Förster, C. (2021). The neuropeptide PDF is crucial for delaying the phase of *Drosophila's* evening neurons under long zeitgeber periods. J. Biol. Rhythms *36*, 442–460.
78. Seluzicki, A., Flourakis, M., Kula-Eversole, E., Zhang, L., Kilman, V., and Allada, R. (2014). Dual PDF signaling pathways reset clocks via TIMELESS and acutely excite target neurons to control circadian behavior. PLoS Biol. *12*, e1001810.
79. Yoshii, T., Wülbeck, C., Sehadova, H., Veleri, S., Bichler, D., Stanewsky, R., and Helfrich-Förster, C. (2009). The neuropeptide pigment-dispersing factor adjusts period and phase of Drosophila's clock. J. Neurosci. *29*, 2597–2610.
80. Ojima, N., Hara, Y., Ito, H., and Yamamoto, D. (2018). Genetic dissection of stress-induced reproductive arrest in Drosophila melanogaster females. PLoS Genet. *14*, e1007434.
81. Nagy, D., Cusumano, P., Andreatta, G., Anduaga, A.M., Hermann-Luibl, C., Reinhard, N., Gesto, J., Wegener, C., Mazzotta, G., Rosato, E., et al. (2019). Peptidergic signaling from clock neurons regulates reproductive dormancy in Drosophila melanogaster. PLoS Genet. *15*, e1008158.
82. Hidalgo, S., Anguiano, M., Tabuloc, C.A., and Chiu, J.C. (2023). Seasonal cues act through the circadian clock and pigment-dispersing factor to control EYES ABSENT and downstream physiological changes. Curr. Biol. *0*. https://doi.org/10.1016/j.cub.2023.01.006.
83. Hasebe, M., Kotaki, T., and Shiga, S. (2022). Pigment-dispersing factor is involved in photoperiodic control of reproduction in the brown-winged green bug, Plautia stali. J. Insect Physiol. *137*, 104359.
84. Kotwica-Rolinska, J., Damulewicz, M., Chodakova, L., Kristofova, L., and Dolezel, D. (2022). Pigment Dispersing Factor Is a Circadian Clock Output and Regulates Photoperiodic Response in the Linden Bug, Pyrrhocoris apterus. Front. Physiol. *13*, 884909.
85. Kaniewska, M.M., Chvalová, D., and Dolezel, D. (2023). Impact of photoperiod and functional clock on male diapause in cryptochrome and pdf mutants in the linden bug Pyrrhocoris apterus. J. Comp. Physiol. A Neuroethol. Sens. Neural Behav. Physiol. https://doi.org/10.1007/s00359-023-01647-5.
86. Beck, S.D., and Hanec, W. (1960). Diapause in the European corn borer, Pyrausta nubilalis (Hübn.). J. Insect Physiol. *4*, 304–318.
87. Mutchmor, J.A., and Beckel, W.E. (1959). Some factors affecting diapause in the European corn borer, O. nubilalis. Preprint, https://doi.org/10.1139/z59-019 https://doi.org/10.1139/z59-019.
88. Pittendrigh, C.S., and Minis, D.H. (1964). The Entrainment of Circadian Oscillations by Light and Their Role as Photoperiodic Clocks. Am. Nat. *98*, 261–294.
89. Yamaguchi, K., and Goto, S.G. (2019). Distinct Physiological Mechanisms Induce Latitudinal and Sexual Differences in the Photoperiodic Induction of Diapause in a Fly. J. Biol. Rhythms *34*, 293–306.
90. Dayton, J.N., and Owens, A.C.S. (2024). iLAM: Imaging Locomotor Activity Monitor for circadian phenotyping of large-bodied flying insects. Methods Ecol. Evol. https://doi.org/10.1111/2041-210x.14403.
91. Barthelmé, S., and Tschumperlé, D. (2019). imager: an R package for image processing based on CImg. J. Open Source Softw. *4*, 1012.
92. Geissmann, Q., Garcia Rodriguez, L., Beckwith, E.J., and Gilestro, G.F. (2019). Rethomics: An R framework to analyse high-throughput behavioural data. PLoS One *14*, e0209331.
93. Borchers, H.W. (2023). Practical Numerical Math Functions [R package pracma version 2.4.4].
94. Dobin, A., Davis, C.A., Schlesinger, F., Drenkow, J., Zaleski, C., Jha, S., Batut, P.,

Chaisson, M., and Gingeras, T.R. (2023). STAR: ultrafast universal RNA-seq aligner. Bioinformatics *29*, 15–21.
95. Ritchie, M.E., Phipson, B., Wu, D., Hu, Y., Law, C.W., Shi, W., and Smyth, G.K. (2015). limma powers differential expression analyses for RNA-sequencing and microarray studies. Nucleic Acids Res. *43*, e47.
96. Parsons, R., Parsons, R., Garner, N., Oster, H., and Rawashdeh, O. (2020). CircaCompare: a method to estimate and statistically support differences in mesor, amplitude and phase, between circadian rhythms. Bioinformatics *36*, 1208–1212.
97. Camacho, C., Coulouris, G., Avagyan, V., Ma, N., Papadopoulos, J., Bealer, K., and Madden, T.L. (2009). BLAST+: architecture and applications. BMC Bioinformatics *10*, 421.
98. Liu, L., Chen, R., Fugina, C.J., Siegel, B., and Jackson, D. (2021). High-throughput and low-cost genotyping method for plant genome editing. Curr. Protoc. *1*, e100.
99. Martin, M. (2011). Cutadapt removes adapter sequences from high-throughput sequencing reads. EMBnet J. *17*, 10.
100. Gaspar, J.M. (2018). NGmerge: merging paired-end reads via novel empirically-derived models of sequencing errors. BMC Bioinformatics *19*, 536.
101. Kim, D., Paggi, J.M., Park, C., Bennett, C., and Salzberg, S.L. (2019). Graph-based genome alignment and genotyping with HISAT2 and HISAT-genotype. Nat. Biotechnol. *37*, 907–915.
102. Danecek, P., Bonfield, J.K., Liddle, J., Marshall, J., Ohan, V., Pollard, M.O., Whitwham, A., Keane, T., McCarthy, S.A., Davies, R.M., et al. (2021). Twelve years of SAMtools and BCFtools. Gigascience *10*, giab008.
103. Poplin, R., Ruano-Rubio, V., DePristo, M.A., Fennell, T.J., Carneiro, M.O., Van der Auwera, G.A., Kling, D.E., Gauthier, L.D., Levy-Moonshine, A., Roazen, D., et al. (2017). Scaling accurate genetic variant discovery to tens of thousands of samples. bioRxiv, 201178. https://doi.org/10.1101/201178.
104. Knaus, B.J., and Grünwald, N.J. (2017). vcfr: a package to manipulate and visualize variant call format data in R. Mol. Ecol. Resour. *17*, 44–53.
105. Pedersen, B.S., Brown, J.M., Dashnow, H., Wallace, A.D., Velinder, M., Tristani-Firouzi, M., Schiffman, J.D., Tvrdik, T., Mao, R., Best, D.H., et al. (2021). Effective variant filtering and expected candidate variant yield in studies of rare human disease. NPJ Genom. Med. *6*, 60.
106. R Core Team (2023). R: A language and environment for statistical computing.
107. Agostinelli, C., and Lund, U. (2024). circular: Circular Statistics (Comprehensive R Archive Network (CRAN)).
108. Fox, J., and Weisberg, S. (2024). Companion to Applied Regression (Comprehensive R Archive Network (CRAN)).

Fig. 1.

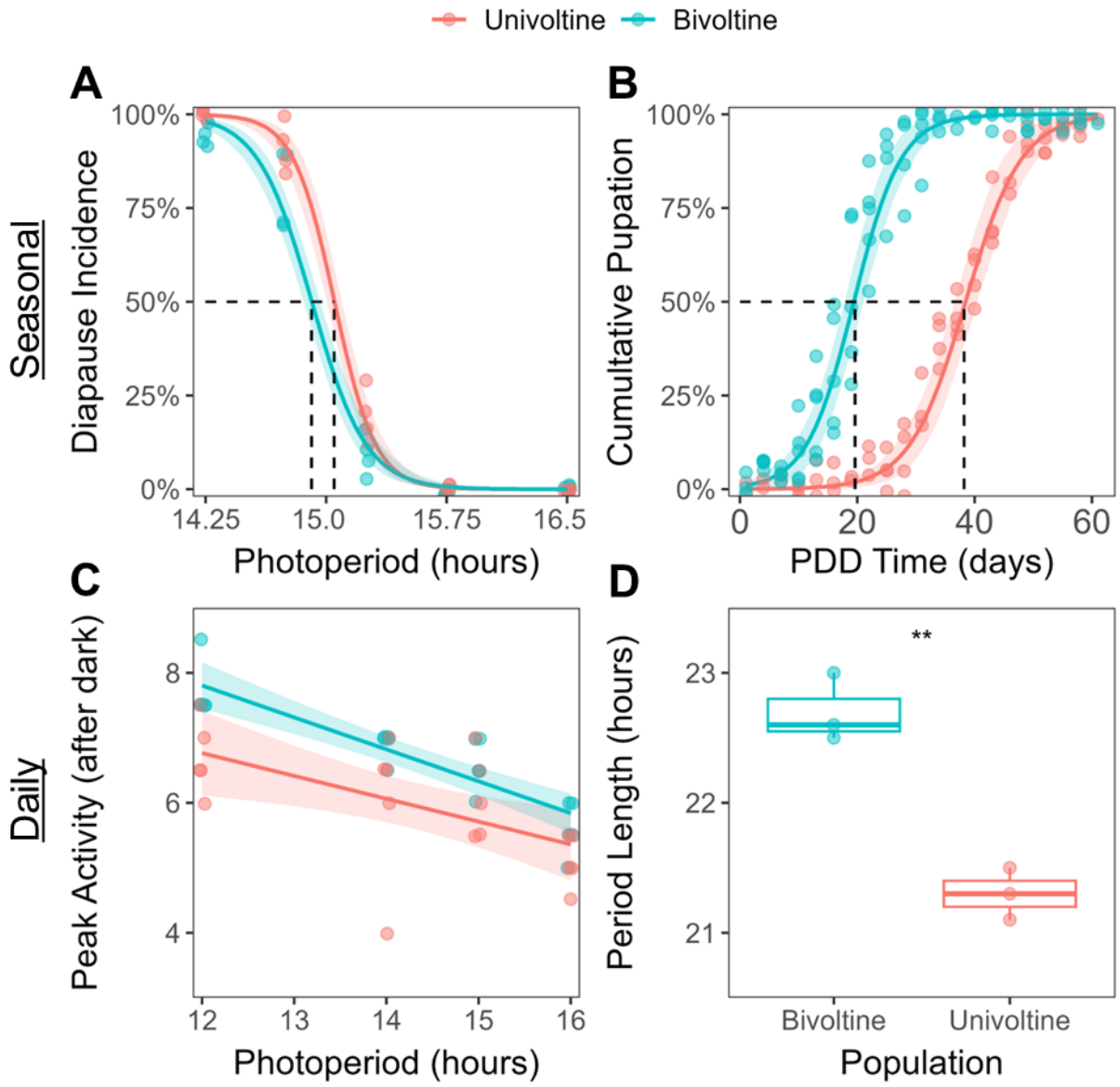

Fig. 2.

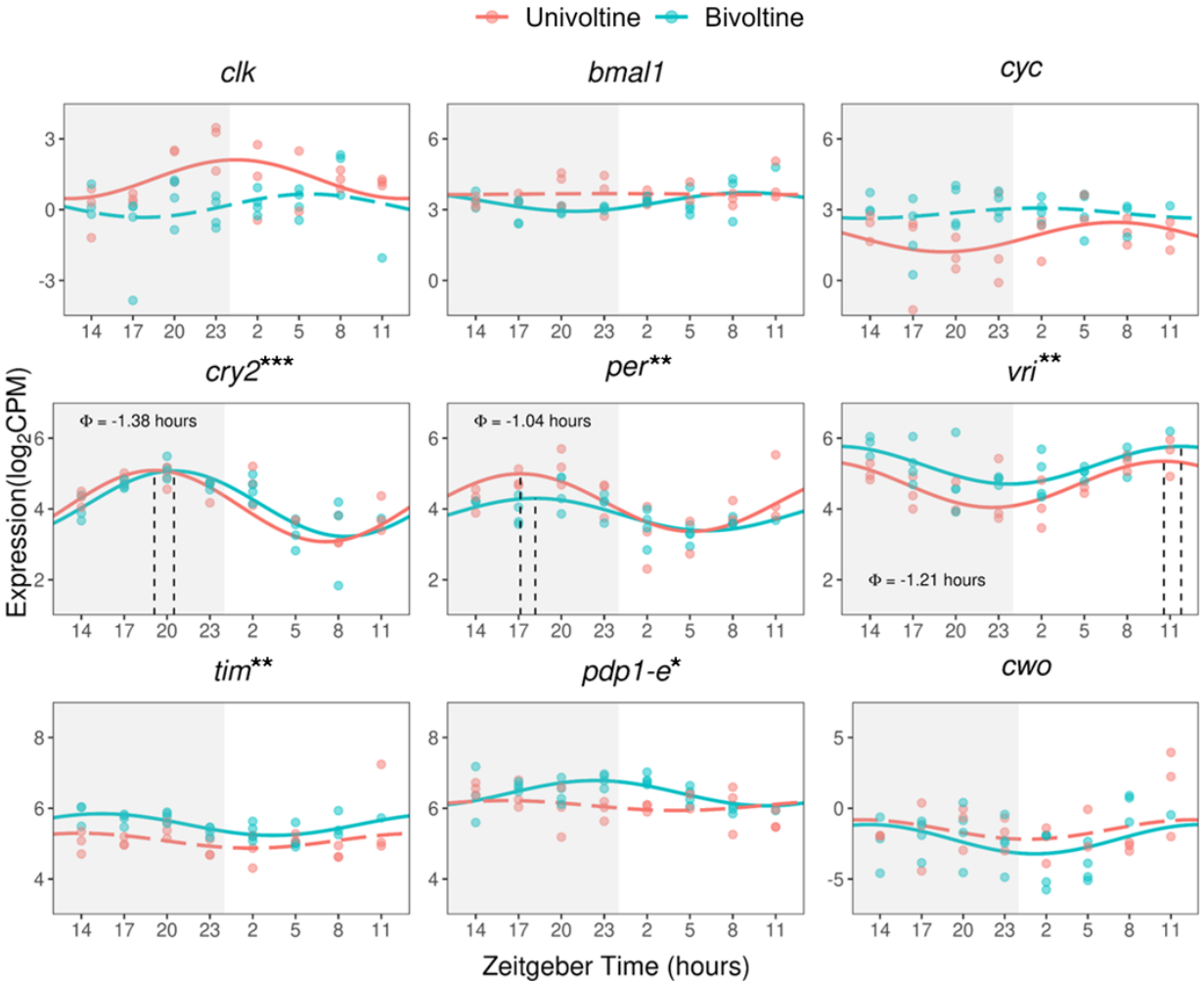

Fig. 3.

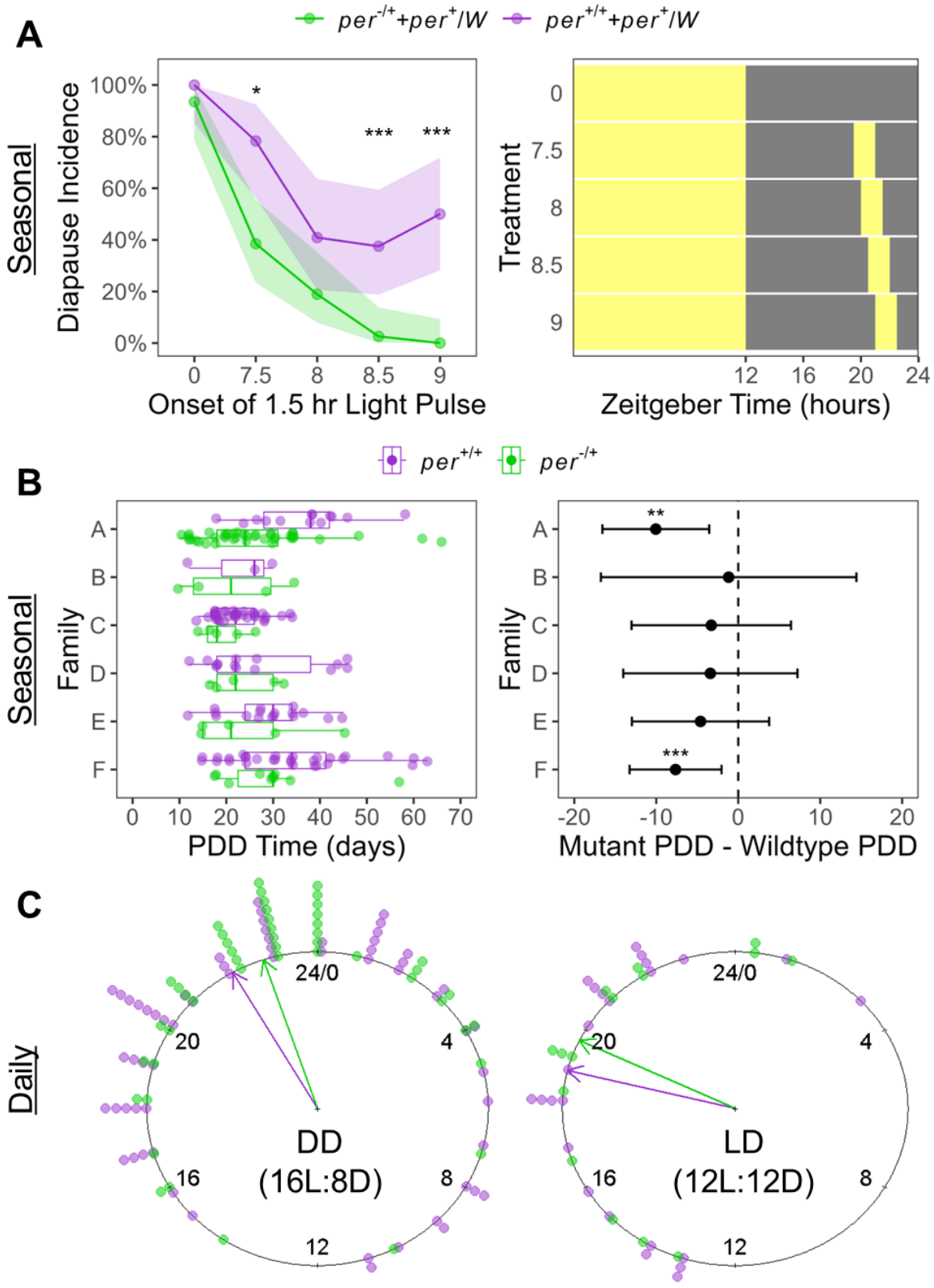

Fig. 4.

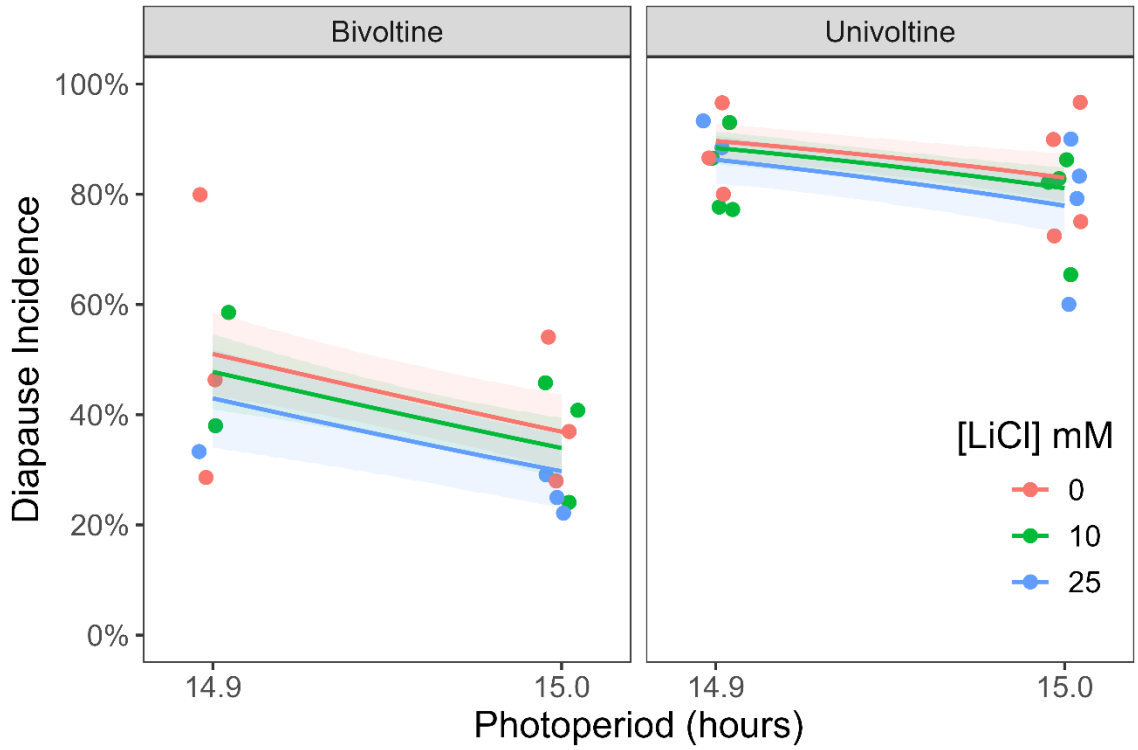

Fig. 5.